Heliyon 10 (2024) e37710

Contents lists available at ScienceDirect

Heliyon

journal homepage: www.cell.com/heliyon

Research article

Exploring the oncogenic potential of Aiolos in lung cancer through OTUB1-mediated ubiquitination

Xiuwen Zhang [a,1], Mei Zhong [a,1], Xinyue Fu [b,1], Hongli Pan [a], Hongyu Liu [a], Jun Chen [a,**], Fengjie Guo [a,b,*]

[a] Tianjin Key Laboratory of Lung Cancer Metastasis and Tumor Microenvironment, Tianjin Lung Cancer Institute, Tianjin Medical University General Hospital, Tianjin, 300052, China
[b] The South China University of Technology School of Medicine, Guangzhou, 510006, China

ARTICLE INFO

Keywords:
Aiolos
OTUB1
Lung cancer
Ubiquitination

ABSTRACT

Aiolos (IKZF3), a zinc finger transcription factor, has been identified in various solid tumors. While most research on Aiolos focuses on its role in the hematopoietic system, its expression patterns, mechanisms of action, and biological impacts in lung cancer remain relatively unexplored. This study investigates Aiolos' role in the proliferation, migration, and invasion of lung cancer cells. Our findings indicate that Aiolos overexpression enhances these cellular processes, suggesting its potential contribution to the advancement of the disease. However, the precise mechanisms underlying these effects require further investigation. Additionally, we identified OTUB1 as a potential Aiolos-interacting protein. OTUB1, a deubiquitinating enzyme, removes ubiquitin chains from target proteins, thereby affecting their stability, function, or localization. Our results suggest that OTUB1 specially bound to Aiolos and reduces its ubiquitination, which may influence Aiolos-related biological functions, including cell migration and invasion. This study highlights the pivotal roles of Aiolos and OTUB1 in lung cancer progression, potentially offering new therapeutic targets.

1. Introduction

Lung cancer is the leading cause of cancer-related deaths both in China and globally. In 2022, it was estimated that China would see around 4.82 million new cancer diagnoses and approximately 3.21 million cancer-related fatalities. Lung cancer ranks as the most prevalent type of cancer in China [1]. On the grounds of histology, the World Health Organization segregates lung cancer into two primary subtypes: Small Cell Lung Cancer (SCLC) and Non-Small Cell Lung Cancer (NSCLC). Among patients, NSCLC is more common and includes several frequent types, such as Lung Squamous Cell Carcinoma (LUSC), Lung Adenocarcinoma (LUAD), and Large Cell Carcinoma (LCC), among others [2,3].

Aiolos, encoded by IKZF3 gene (Ikaros Family Zinc Finger 3), is a transcription factor, characterized by a zinc finger, and is part of the Ikaros family, which includes Ikaros, Helios, Eos, and Pegasus [4]. Aiolos is predominantly found in peripheral blood lymphocytes, spleen, and thymus tissue, where it plays a crucial role in lymphocyte development [5]. Although Aiolos expression has been observed

* Corresponding author. South China University of Technology, Guangzhou, 510006, China.
** Corresponding author.
E-mail addresses: huntercj2004@yahoo.com (J. Chen), guofengjie@scut.edu.cn (F. Guo).
[1] Xiuwen Zhang, Mei Zhong and Xinyue Fu contributed equally to this work.

https://doi.org/10.1016/j.heliyon.2024.e37710
Received 9 June 2024; Received in revised form 30 August 2024; Accepted 9 September 2024
Available online 10 September 2024

in various solid tumors, including those in lung, breast, and colon, most research has focused on its role in the hematopoietic system [6–8]. Recently, studies have started to investigate Aiolos' role in solid tumors, including lung cancer [9]. Notably, recent research has highlighted its potential role in lung cancer, particularly as an epigenetic driver of lymphocyte mimicry that links immune cell development to metastatic behavior [10]. Aiolos has been shown to enhance cancer stem cell like characteristics and promote epithelial-mesenchymal transition in lung cancer cells [11]. However, the understanding of its expression patterns, mechanisms of action, and biological impact specifically in lung cancer remains limited.

OTUB1 is a deubiquitinating enzyme (DUB) that removes ubiquitin from target proteins, preventing their degradation by the proteasome [12]. By regulating the degradation of proteins involved in cell cycle regulation and apoptosis, OTUB1 can influence the growth and metastasis of cancer tumors. Understanding these pathways could help identify new biomarkers for disease progression.

In this study, we propose that Aiolos overexpression enhances migratory and invasive abilities in lung cancer cells, potentially contributing to metastasis. We also identify OTUB1 as an Aiolos-interacting protein that appears to reduce Aiolos' ubiquitination, thereby influencing cell migration and invasion. Consequently, Aiolos and OTUB1 might be pivotal in lung cancer progression and serve as potential treatment targets.

2. Material and methods

2.1. Bioinformatics methods

In this study, we utilized UALCAN (The University of ALabama at Birmingham CANcer data analysis Portal), an online resource designed for analyzing TCGA pan-cancer datasets, accessible at https://ualcan.path.uab.edu/. This tool facilitated comprehensive data exploration and analysis of Aiolos (IKZF3) expression across multiple cancer types. Statistical computations and data visualization were performed using R version 4.1.2, taking advantage of its robust capabilities for data handling and graphical representation. Specifically, to account for non-normally distributed paired samples, we employed the Wilcoxon signed-rank test.

2.2. Cell cultures

Human lung cancer A549 and human embryonic kidney 293T cells were obtained from ATCC and cultured in Dulbecco's Modified Eagle Medium (DMEM, Gibco) supplemented with 10 % fetal bovine serum (Gibco), 100 U/mL penicillin, and 100 μg/mL streptomycin (Gibco). H1299 and H1975 human lung cancer cells were maintained in RPMI-1640 Medium (Gibco) supplemented with 10 % fetal bovine serum, 100 U/mL penicillin, and 100 μg/mL streptomycin. The cells were incubated at 37 °C in a 5 % CO2 atmosphere.

2.3. Cell transfection

Cell transfection was carried out using Lipofectamine 2000 transfection reagent (Thermo Fisher Scientific). Briefly, the day before transfection, cells were seeded into culture vessels at an appropriate density. On the day of transfection, plasmid DNA and Lipofectamine 2000 transfection reagent were separately diluted in Opti-MEM (Gibco) and incubated for 5 min. Subsequently, the diluted DNA and Lipofectamine 2000 were gently mixed together and allowed to incubate for 20–30 min to form transfection complexes. The growth medium was removed from the cells and replaced with fresh culture medium without antibiotics. The transfection complexes were added to the cells. The cells were then incubated at 37 °C in a 5 % CO2 atmosphere to perform downstream assays.

2.4. Quantitative reverse transcription PCR (qRT-PCR)

Quantitative Reverse Transcription Polymerase Chain Reaction (qRT-PCR) was performed following a defined protocol, basically as described in the literature [13]. Total RNA was isolated from the respective cells or tissues utilizing TRIzol reagent (Thermo Fisher Scientific). The isolated RNA was subsequently transcribed into complementary DNA (cDNA) using a reverse transcription kit (Thermo Fisher Scientific). The cDNA was subjected to quantitative PCR with specific primers for each target gene and an appropriate SYBR Green qPCR master mix (Thermo Fisher Scientific). Relative expression levels of each gene were calculated using the 2^-ΔΔCt method, with GAPDH serving as an endogenous control for normalization. All experiments were conducted in triplicate to guarantee data accuracy and reliability.

The sequences of the primers designated to amplify the Aiolos gene were:

Forward: 5′-GCTCATACAGACCCGCATGAT-3′

Reverse: 5′-AACTGGAACCATCTCCGAGGT-3′.

2.5. Immunochemistry

The immunohistochemistry protocol was executed with modifications based on a previously described method [14]. The slides were initially deparaffinized using xylene and then rehydrated through a series of graded alcohols. Antigen retrieval was performed by immersing the sections in citrate buffer and applying heat. The sections were then treated with 3 % hydrogen peroxide to block endogenous peroxidase activity. Following this, the sections were incubated with an anti-Aiolos antibody (Cell Signaling Technology) overnight at 4 °C. The primary antibody was then washed off, and a secondary antibody (Cell Signaling Technology) was applied and incubated at room temperature for 1 h. The sections were subsequently treated with a streptavidin-horseradish peroxidase complex

and developed with a diaminobenzidine substrate for color visualization. Counterstaining was performed using hematoxylin, followed by dehydration through graded alcohols and clearing with xylene. The slides were then prepared for microscopic examination to analyze the distribution and localization of the target protein in the samples.

2.6. Western blot

The Western blot assay was conducted to confirm the expression levels of the target proteins. To summarize the process, cells were harvested and lysed using RIPA buffer to release proteins. Protein concentration was measured using a bicinchoninic acid (BCA) assay. Cellular protein lysates underwent sodium dodecyl sulfate-polyacrylamide gel electrophoresis (SDS-PAGE) and were subsequently transferred to a nitrocellulose membrane. The membrane was blocked with a suitable blocking buffer, followed by incubation with primary antibodies at 4 °C overnight. The primary antibodies used included Aiolos (15103, Cell Signaling Technology), V5-tag (13202, Cell Signaling Technology), Flag-tag (F3165, Sigma-Aldrich), and GAPDH (sc-32233, Santa Cruz Biotechnology). After thorough washing, the membrane was incubated with horseradish peroxidase-conjugated secondary antibodies. Protein bands were visualized using an enhanced chemiluminescence detection system.

2.7. CCK-8 assay

Cell proliferation was assessed using the CCK-8 method as described elsewhere [15]. Cells were plated into 96-well plates at a density of 5000 cells per well and allowed to grow overnight in a CO_2 incubator at 37 °C. Cells were then treated and incubated for the desired duration. After the incubation period, each well was treated with 10 μLof CCK-8 solution (Sigma-Aldrich) and incubated for an additional 2 h at 37 °C. Absorbance at 450 nm was measured using a microplate reader. This procedure was repeated at various intervals to track cell proliferation. Each experiment was repeated three times to ensure consistency.

2.8. Wound healing assay

A wound healing assay, a critical tool for investigating cell migration, was conducted following a streamlined process [16]. Cells are cultured in a dish and incubated under appropriate conditions until they reach 70–90 % confluence. A sterile pipette tip is used to create a wound across the cell monolayer. The dish was then gently rinsed to eliminate any dislodged cells, and fresh complete medium was added. The initial wound was imaged using an inverted microscope to establish a 0-h reference point. Additional images of the wound area are captured every 24 h. The wound area at each time interval was calculated using ImageJ analysis software, allowing for a comparative analysis of the wound healing rate. The data were normalized to the initial scratch area at time 0. The area recovery percentage was calculated using the formula: Area recovery (%) = (Initial scratch area - Scratch area at time t)/Initial scratch area.

2.9. Transwell assay

Cell migration and invasion were determined using Transwell chambers (Corning, USA) as described elsewhere with some modification [17]. Cells were collected, quantified, and resuspended in a medium without serum. A count of $1 \times 10\hat{}5$ cells in 200 μL of this serum-free medium was added to the upper chamber of each well. The lower chamber was filled with 600 μL of medium supplemented with 10 % serum to act as a chemoattractant. The plates were incubated at 37 °C in a 5 % CO_2 environment for 24 h to allow for cell migration and invasion. After incubation, cells remaining on the upper surface of the membrane were gently wiped off with a cotton swab. Cells that had migrated or invaded to the lower surface of the membrane were fixed using 4 % paraformaldehyde and stained with 0.1 % crystal violet. The membrane was gently washed with PBS to remove excess stain. The number of migrated or invaded cells on the lower membrane surface was quantified under a light microscope in five randomly chosen fields per well.

2.10. Co-immunoprecipitation (Co-IP)

Co-immunoprecipitation (Co-IP) is used to study protein-protein interactions as previously described [18]. Cells were harvested and lysed using a lysis buffer. The cell lysate was centrifuged to remove debris, leaving the protein-rich supernatant. Protein G agarose was added to the lysate and incubated on a rotator for 1 h at 4 °C to reduce non-specific binding. Agarose was removed by centrifugation, and the supernatant was transferred to a new tube. An antibody specific to the target protein was added to the lysate and incubated overnight at 4 °C. Following incubation, protein G agarose (Thermo Fisher Scientific) was added and incubated for another 2 h at 4 °C. The mixture was centrifuged to pellet the agarose, which was then washed with a cold IP buffer. The protein was eluted from the agarose by adding a sample buffer and boiling the sample. Finally, the eluted protein sample was run on an SDS-PAGE gel and subjected to Western blotting.

2.11. Cycloheximide (CHX) pulse-chase assay

The CHX pulse-chase assay is used to study protein stability and degradation rates. Cells were plated onto 12-well plates at a density of 1×10^5 cells per well and allowed to adhere overnight under standard culture conditions. After cellular attachment, cells were transfected with plasmid vectors. Twenty-four hours post-transfection, protein synthesis was blocked using a cycloheximide (CHX) (Sigma-Aldrich) treatment at a concentration of 100 μg/mL. The lysates were analyzed by western blotting using an anti-FLAG (Aiolos)

antibody to determine the relative abundance of Aiolos protein over time. Appropriate loading controls were included to normalize protein levels. Normalized protein levels were plotted against time to create a degradation curve. Each experiment was repeated three times.

2.12. Ubiquitination assay

Ubiquitination assays were conducted to study protein ubiquitination as previously described [18]. Briefly, cells were transfected with applicable plasmids, including HA-ubiquitin (HA-ub). After 24 h, cells were treated with the proteasome inhibitor MG132 (Sigma-Aldrich) for 4 h before harvest. Cells were then lysed in an SDS lysis buffer (2 % SDS, 150 mM sodium chloride, 10 mM Tris, pH 8.0). The lysates were incubated overnight at 4 °C with the primary antibody, followed by incubation with protein G agarose for 2 h at 4 °C. The immunoprecipitated proteins were washed three times with the lysis buffer and eluted via boiling in SDS sample buffer for 5 min. The sample was analyzed by a Western blot.

2.13. Statistical analysis

Each experiment was performed in triplicate, and the entire procedure was independently replicated three times. Data are represented as the mean ± standard deviation (SD). Statistical evaluations were performed using the Student's t-test, with a p-value <0.05 considered statistically significant. In bioinformatics methods, for paired samples that are not normally distributed, we utilized the Wilcoxon signed-rank test.

3. Results

3.1. The expression of Aiolos in lung cancer

In this study, we examined the expression of Aiolos (IKZF3) in lung cancer tissues using bioinformatics techniques to analyze Aiolos data from the TCGA database The results are presented in Fig. 1. Our findings indicate that Aiolos is expressed in several cancer types, including gastric cancer, lung adenocarcinoma, lung squamous cell carcinoma, and esophageal cancer (Fig. 1A). Specifically, Aiolos expression was significantly higher in adenocarcinoma tissues compared to normal tissues. Conversely, squamous cell carcinoma tissues showed lower Aiolos expression levels compared to normal tissues. This discrepancy can be attributed to the distinct biological characteristics and genetic backgrounds of these two tumor types. We analyzed transcriptome data from 469 cases of lung cancer and their corresponding adjacent tissues, revealing elevated Aiolos expression in the tumor tissues (Fig. 1B and C). These findings suggest that Aiolos may have different functional roles in various tumor types, necessitating further investigation.

We conducted real-time quantitative PCR (qPCR) analysis on lung cancer tissues and lung cancer cell lines. The results revealed significantly higher transcript levels of Aiolos in lung cancer tissues compared to adjacent tissues, where either no transcript or low levels were detected (Fig. 1D). This observation indicates a significant difference in Aiolos expression between the two tissue types. Additionally, the qPCR analysis of paired lung cancer and adjacent tissues displayed a consistent distribution pattern of Aiolos transcripts (Fig. 1E). We also observed variations in Aiolos transcript levels among different lung cancer cell lines (Fig. 1F). Notably, the H1299 and H1975 lung cancer cell lines exhibited significantly higher Aiolos transcript levels compared to other lung cancer cell lines. These findings provide valuable insights for the selection of appropriate cell lines for subsequent investigations.

Further immunohistochemical staining of paraffin-embedded sections confirmed the expression of Aiolos in lung cancer tissues at the protein level, revealing significant differences between lung cancer tissues and adjacent tissues. Aiolos was widely expressed in various subtypes of non-small cell lung cancer (NSCLC), including large cell carcinoma (LCC), adenocarcinoma (LUAD), and squamous cell carcinoma (LUSC), both in the cytoplasm and nucleus. However, in small cell lung cancer (SCLC), Aiolos was predominantly localized in the nucleus. Adjacent tissues of large cell carcinoma and lung squamous cell carcinoma exhibited low Aiolos expression, with large cell carcinoma showing more prominent expression (Fig. 1G). The findings suggest that Aiolos may play a key role in the progression of lung cancer.

3.2. Modulation of Aiolos expression affects lung cancer cell proliferation

To further investigate the role of Aiolos in lung cancer, we transfected A549 and H1299 lung cancer cells with Aiolos expression plasmids. Western blot analysis demonstrated an effective induction of Aiolos expression in the experimental group compared to the control group (Fig. 2A). Additionally, we performed knockdown experiments targeting Aiolos in H1299 and H1975 cells, which resulted in a notable reduction in Aiolos protein expression relative to the control group (Fig. 2B). In the CCK-8 cell proliferation assay, we observed a positive correlation between Aiolos expression and cell proliferation capacity. Specifically, overexpression of Aiolos significantly enhanced cell proliferation (Fig. 2C). Conversely, the knockdown of Aiolos in the cells led to a reduction in cell proliferation capacity, exhibiting an opposite trend (Fig. 2D). These findings suggest that Aiolos plays a crucial role in lung cancer cell proliferation.

3.3. The effect of Aiolos on lung cancer cell migration ability

To examine the functional role of Aiolos in cellular migration, we conducted a wound healing assay. Comparative analysis with the

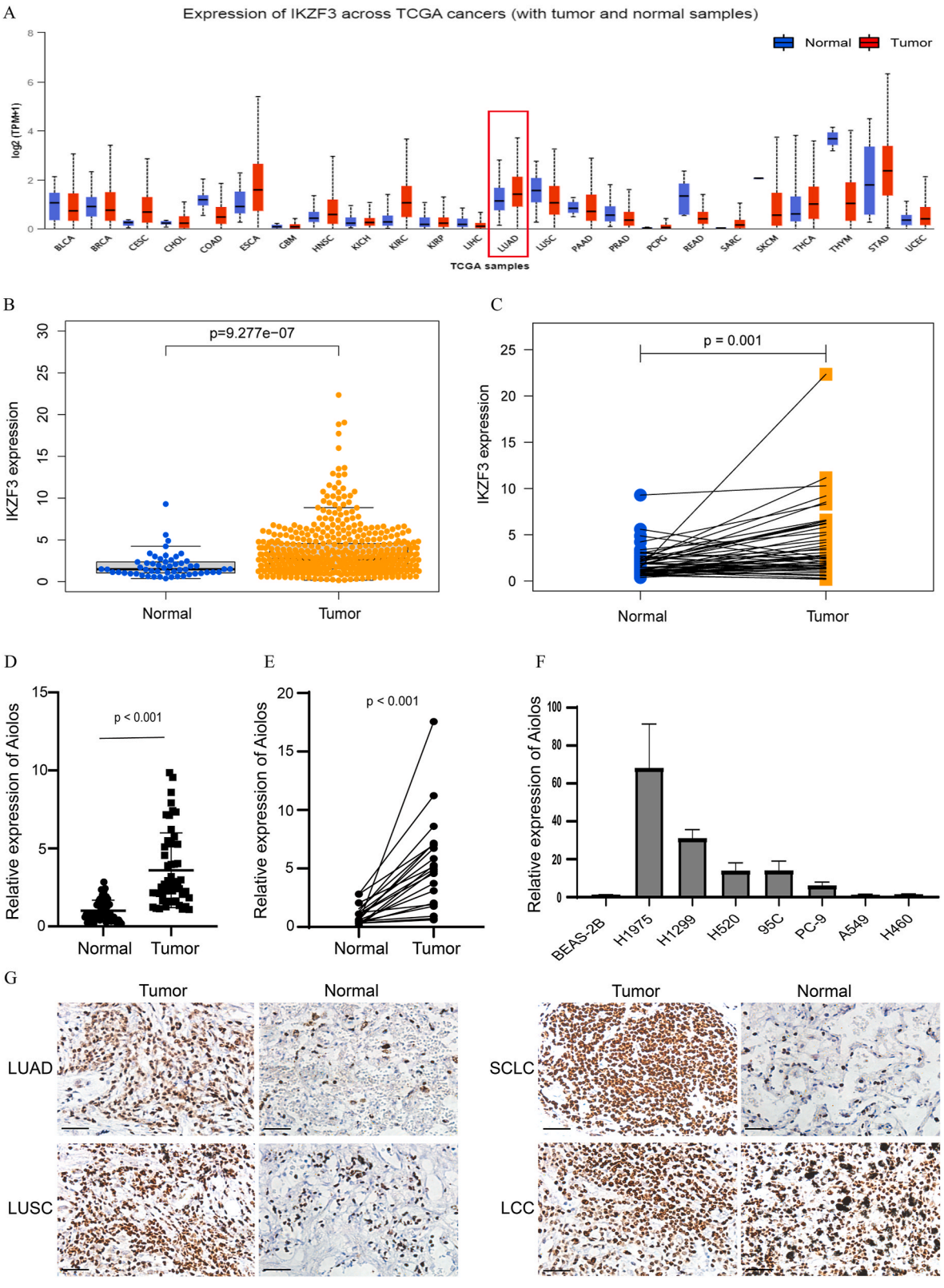

(caption on next page)

Fig. 1. Aiolos expression in lung cancer tissues and cell lines. (A) Boxplot showing the relative expression levels of Aiolos (IKZF3) across various cancer types, comparing tumor and normal samples from the TCGA database. BLCA: bladder urothelial carcinoma. BRCA: breast invasive carcinoma. CESC: cervical squamous cell carcinoma and endocervical adenocarcinoma. CHOL: cholangiocarcinoma. COAD: colon adenocarcinoma. KICH: Kidney Chromophobe. ESCA: esophageal cancer. GBM: glioblastoma multiforme. HNSC: Head and Neck squamous cell carcinoma. KICH: Kidney Chromophobe. KIRC: Kidney renal clear cell carcinoma. KIRP: Kidney renal papillary cell carcinoma. LIHC: Liver hepatocellular carcinoma. LUAD: Lung adenocarcinoma. LUSC: Lung squamous cell carcinoma. PAAD: Pancreatic adenocarcinoma. PCPG: Pheochromocytoma and Paraganglioma. PRAD: Prostate adenocarcinoma. READ: Rectum adenocarcinoma. SARC: Sarcoma. SKCM: Skin Cutaneous Melanoma. TGCT: Testicular Germ Cell Tumors. THCA: Thyroid carcinoma. THYM: Thymoma. STAD: Stomach adenocarcinoma. UCEC: Uterine Corpus Endometrial Carcinoma. (B) Scatter plot representing the differential expression of Aiolos in lung cancer (Tumor) compared to adjacent normal tissues (Normal). (C) Paired analysis line graphs of Aiolos expression between lung adenocarcinoma tissues (Tumor) versus adjacent non-tumor lung tissues (Normal), illustrating individual patient data points. (D) Real-time quantitative PCR (qPCR) analysis results of Aiolos transcript levels in lung cancer tissues (Tumor) versus adjacent normal tissues (Normal). (E) The diagram illustrating the distribution of Aiolos transcript levels in paired lung cancer tissues and adjacent normal tissues, emphasizing variations among patients. (F) Comparative bar chart of Aiolos transcript levels across various lung cancer cell lines, highlighting differences among cell lines. (G) Immunohistochemical staining showed Aiolos protein localization and expression levels in NSCLC subtypes (Large cell carcinoma (LCC), Lung adenocarcinoma (LUAD), and Lung squamous cell carcinoma (LUSC)) and small cell lung cancer (SCLC), as well as in adjacent non-tumor tissues. Scale bar: 50 μm. Statistical evaluations were done using the Student's t-test, with a p-value <0.05 considered statistically significant.

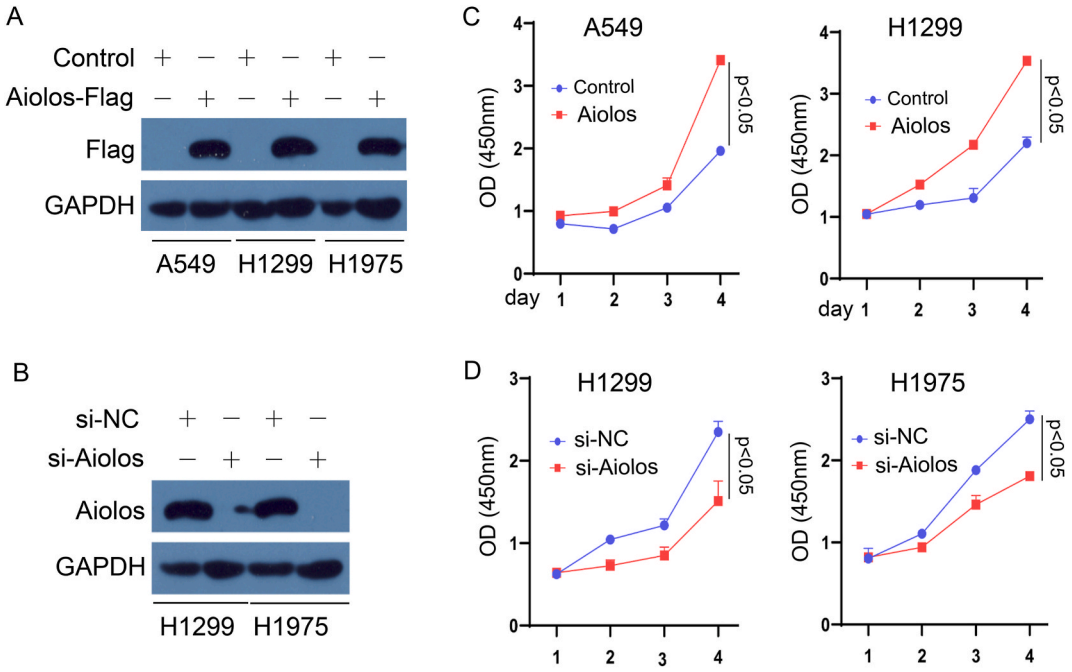

Fig. 2. Modulation of Aiolos expression affects lung cancer cell proliferation. A CCK-8 (Cell Counting Kit-8, CCK-8) assay was used to determine the effect of Aiolos on cell proliferation capacity. (A) Western blot analysis of Aiolos protein levels in A549 and H1299 lung cancer cell lines following transfection with Aiolos expression plasmids, indicating successful overexpression. (B) Western blot analysis demonstrating the effects of Aiolos-targeted knockdown on its protein expression in H1299 and H1975 lung cancer cells post-siRNA transfection. (C) Graph depicting the results of a CCK-8 cell proliferation assay following Aiolos overexpression in A549 and H1299 cells, showing enhanced proliferation. (D) Graph illustrating the impact of Aiolos knockdown on cell proliferation in H1299 and H1975 cells, as assessed by CCK-8 assays, indicating reduced proliferation. Statistical evaluations were done using the Student's t-test. *$P < 0.05$.

control group revealed that overexpression of Aiolos significantly enhanced cell migration capacity (Fig. 3A). Conversely, the knockdown of Aiolos resulted in a significant reduction in cell migration capacity (Fig. 3B). These alterations in migration capacity were further validated by the Transwell migration assay (Fig. 3C and D). In the experiment evaluating cellular invasion capacity, we observed that overexpression of Aiolos significantly enhanced the ability of cells to invade, whereas knockdown of Aiolos resulted in a significant reduction in this invasive capacity (Fig. 3E and F). These results suggest that Aiolos significantly influences both the migration and invasion abilities of lung cancer cells, highlighting its potential role in lung cancer progression.

3.4. The interaction of OTUB1 with Aiolos and its impact on ubiquitination

Given the significant impact of Aiolos on the phenotypic traits of lung cancer cells, we sought to investigate the proteins that interact with Aiolos to better understand its regulatory mechanisms. We performed a Co-Immunoprecipitation (Co-IP) assay using an

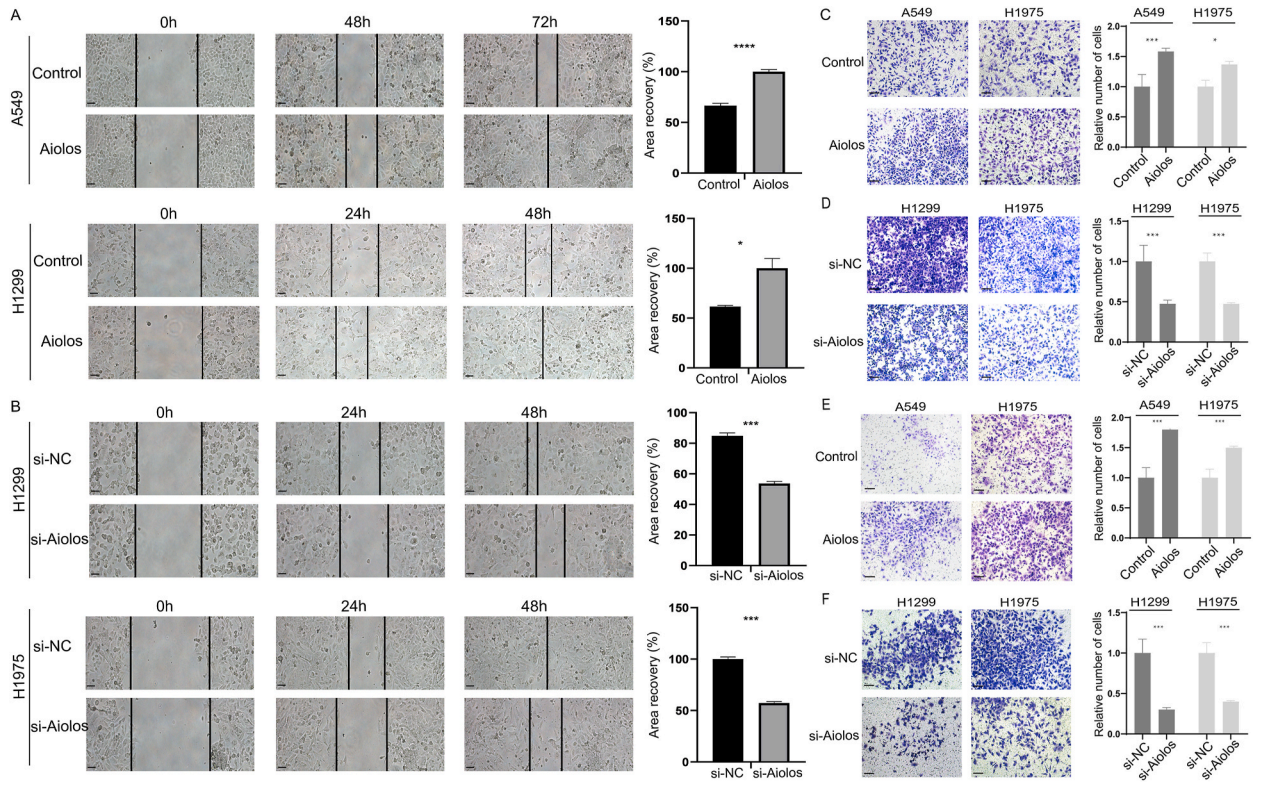

Fig. 3. The Effect of Aiolos on lung cancer cell migration ability. Both wound healing and transwell assay were used to detect cell migration. (A) Wound healing assay demonstrating increased migration of A549 and H1299 lung cancer cells overexpressing Aiolos compared to control plasmid. The right panel shows the percentage of wound closure over time, indicating enhanced migratory capacity. Control: empty plasmid control. Aiolos: Aiolos-expressing plasmid. (B) Wound healing assay showing decreased migration of H1299 and H1975 lung cancer cells with Aiolos knockdown. The right panel depicts the percentage of wound closure, indicating reduced migration. si-NC: small interfering RNA Negative Control. si-Aiolos: small interfering RNA targeting Aiolos. (C) Transwell migration assay results for A549 and H1975 lung cancer cells transfected with Aiolos expression plasmid and the corresponding control plasmid. The representative images and quantitative analysis indicate the number of migrated cells per field, showing increased migration with Aiolos overexpression. (D) Transwell migration assay results for H1299 and H1975 lung cancer cells with Aiolos knockdown. The images and accompanying graph quantify the number of cells that migrated through the membrane, showing decreased migration with Aiolos knockdown. (E) Invasion assay findings for A549 and H1975 lung cancer cells overexpressing Aiolos. Representative micrographs and the graph below demonstrate the number of cells invading through the Matrigel to the lower chamber, indicating enhanced invasive capacity. (F) Invasion assay results for H1299 and H1975 lung cancer cells after Aiolos knockdown. The images and graph represent the reduced number of invasive cells compared to control, indicating decreased invasive ability. Statistical evaluations were performed using the Student's t-test. $^{*}P < 0.05$, $^{***}P < 0.001$, $^{****}P < 0.0001$. Scale bar: 100 μm.

anti-Flag antibody in 293T cells transfected with Aiolos-Flag. Following immunoprecipitation, the proteins bound to Aiolos were separated by SDS-PAGE and analyzed by Mass Spectrometry (MS). This analysis identified OTUB1 as a potential interacting protein with Aiolos (Fig. 4A). To confirm this interaction, we conducted an additional Co-IP assay, which validated the binding of OTUB1 to Aiolos (Fig. 4B). OTUB1 is a deubiquitinating enzyme (DUB) to remove ubiquitin chains from target proteins, affecting their stability, function, or localization [19]. Our experiments showed a notable increase in Aiolos protein levels following transfection with OTUB1, suggesting that OTUB1 may stabilize Aiolos (Fig. 4C). Further analysis using the cycloheximide (CHX) pulse-chase assay indicated enhanced stability of the Aiolos protein in cells overexpressing OTUB1 (Fig. 4C and D). Additionally, we observed a significant decrease in Aiolos ubiquitination levels in the presence of elevated OTUB1 (Fig. 4E). These findings suggest that OTUB1 interacts with Aiolos and regulates its ubiquitination, thereby influencing Aiolos protein stability. This interaction presents a novel post-translational regulatory mechanism that warrants further investigation to understand its role in lung cancer progression.

4. Discussion

Aiolosis is a protein crucial for the regulation of immune cell proliferation and function. It belongs to the Ikaros family of proteins, which are typically involved in transcription regulation by binding to specific DNA sequences and controlling the transcription of genetic information from DNA to RNA [20–22]. Loss-of-function variants in AIOLOS lead to varying degrees of immunodeficiency and immune dysregulation, with different molecular mechanisms and clinical phenotypes observed, including a new autosomal dominant mechanism caused by heterodimeric interference with IKAROS [23–25]. Additionally, germline IKZF2 mutations in patients with

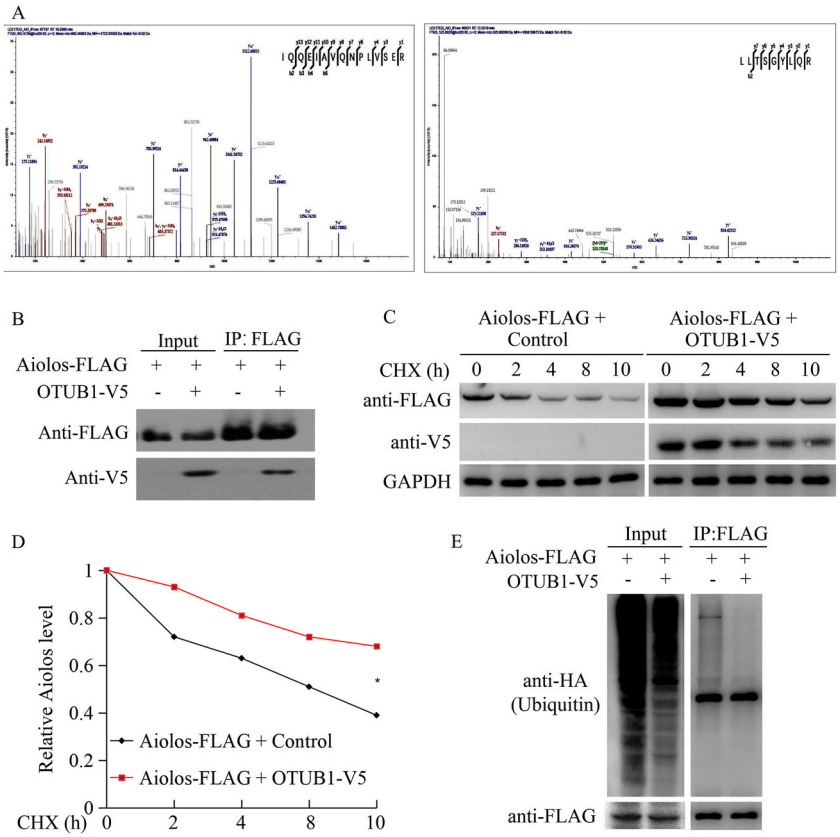

Fig. 4. The interaction of OTUB1 with Aiolos and its impact on ubiquitination. (A) Aiolos-Flag was immunoprecipitated from 293T cell lysates using an anti-Flag antibody. The proteins pulled down were resolved into bands and analyzed by Mass Spectrometry, leading to the identification of OTUB1 as a candidate interacting partner of Aiolos, as indicated by the specific peptide fragments detected. (B) Validation of the Aiolos-OTUB1 interaction by Co-immunoprecipitation assay. Immunoblots showing the expression of the indicated protein confirm the interaction. V5: a V5 epitope tag. (C) 293T cells were cotransfected with Aiolos and either OTUB1 or a control vector, followed by a cycloheximide (CHX) pulse-chase assay to assess the stability of Aiolos protein over time. (D) Quantitative analysis of Western blot data from the CHX pulse-chase assay, showing the degradation rate of Aiolos in the presence of OTUB1 compared to control. (E) Assessment of Aiolos ubiquitination levels through co-immunoprecipitation (co-IP) following cotransfection of OTUB1 or a control vector with Aiolos and HA-tagged ubiquitin into 293T cells. Statistical evaluations were performed using the Student's t-test. $^{*}P < 0.05$.

systemic lupus erythematosus and related disorders result in hypogammaglobulinemia and disrupted T-cell function due to impaired homodimerization, DNA binding, and aberrant interactions with the NuRD complex, causing epigenetic and transcriptional dysregulation [26].

The role of Aiolos in oncogenesis is still under investigation. However, emerging evidence suggests a potential connection between Aiolos and certain types of cancer due to its role in the Ikaros family [27,28]. The expression of Aiolos has been linked to survival in some hematological cancers, including multiple myeloma and acute lymphoblastic leukemia [29,30].

However, the relationship between Aiolos and lung cancer remains largely unexplored in recent studies [10]. This study aims to shed light on this relationship and explore the potential role of Aiolos in lung cancer. Our findings emphasize the crucial role of Aiolos in the migration and invasion ability of lung cancer cells. Overexpression of Aiolos notably enhanced the migratory and invasive capacity of these cells, while its knockdown considerably reduced these abilities. This suggests that Aiolos could potentially be a significant factor in the metastasis of lung cancer, further demonstrating the importance of understanding the molecular mechanisms of its regulation.

While Aiolos belongs to a transcription factor family known for regulating the expression and function of its targets, research investigating the manipulation of Aiolos expression in lung cancer cells has been limited [31]. Our study extended to the identification of proteins that interact with Aiolos, where we discovered OTUB1 as a potential interacting partner. Deubiquitinating enzyme OTUB1 is crucial in the DNA damage response, stabilizing key proteins such as p53 and BRCA1, and preserving genomic integrity. It also regulates various signaling pathways, including the NF-κB pathway, by deubiquitinating and stabilizing their components, which is vital for cell growth and differentiation. Given its significant role in cancer biology, OTUB1 is seen as a potential therapeutic target. Modulating its activity could improve cancer treatments by promoting the degradation of oncogenic proteins or stabilizing tumor suppressors. Our results demonstrated that OTUB1 effectively reduced the ubiquitination of Aiolos, thereby enhancing its stability.

This suggests that Aiolos could be a potential target in lung cancer therapy.

These findings are significant since ubiquitination is a crucial post-translational modification that controls protein degradation, cellular processes, and signaling pathways. Thus, OTUB1's interaction with Aiolos could potentially impact the protein's function, stability, or intracellular location. This could further influence the biological functions associated with Aiolos, including cell migration and invasion. Lenalidomide and Pomalidomide, as Immunomodulatory Drugs (IMiDs), have been used in hematologic malignancies and have shown efficacy in degrading Aiolos. They modulate the immune response and can target transcription factors like Aiolos, leading to its degradation via the ubiquitin-proteasome pathway. These IMiDs hold promise for lung cancer treatment.

However, the precise mechanism of how OTUB1's deubiquitination of Aiolos affects the latter's function and subsequent cell behaviors remains unclear and warrants further investigation. Unraveling this mechanism could provide valuable insights into the regulation of lung cancer cell migration and invasion. Furthermore, Aiolos and OTUB1 represent promising therapeutic targets in cancer treatment. While Aiolos can be targeted by existing IMiDs, further research is needed to develop specific inhibitors for both Aiolos and OTUB1.

In conclusion, our findings highlight the crucial role of Aiolos in lung cancer cell migration and invasion, and the potential regulatory role of OTUB1 on Aiolos through deubiquitination. Our study contributes to the understanding of the molecular mechanisms underlying lung cancer progression and might provide potential therapeutic targets.

Ethics approval and consent to participate

This study protocol was approved by the Medical Ethics Committee of Tianjin Medical University General Hospital (IRB-2020-KY-007) (January 23, 2020) and followed the Declaration of Helsinki. The ethics committee granted a waiver of consent from individual participants.

Data availability statement

Data included in article/material/referenced in article.

CRediT authorship contribution statement

Xiuwen Zhang: Methodology, Investigation, Data curation. **Mei Zhong:** Methodology, Investigation, Formal analysis. **Xinyue Fu:** Methodology, Investigation. **Hongli Pan:** Methodology, Investigation. **Hongyu Liu:** Methodology, Investigation. **Jun Chen:** Writing – review & editing, Supervision, Resources, Formal analysis, Data curation. **Fengjie Guo:** Writing – original draft, Supervision, Resources, Project administration, Funding acquisition, Formal analysis, Data curation, Conceptualization.

Declaration of competing interest

The authors have no conflicts of interest.

Acknowledgements

This work was financially supported by National Natural Science Foundation of China (No.82070214).

References

[1] C. Xia, et al., Cancer statistics in China and United States, 2022: profiles, trends, and determinants, Chin. Med. J. 135 (2022) 584–590, https://doi.org/10.1097/CM9.0000000000002108.
[2] N. Coudray, et al., Classification and mutation prediction from non-small cell lung cancer histopathology images using deep learning, Nat. Med. 24 (2018) 1559–1567, https://doi.org/10.1038/s41591-018-0177-5.
[3] Y. Han, et al., Histologic subtype classification of non-small cell lung cancer using PET/CT images, Eur. J. Nucl. Med. Mol. Imag. 48 (2021) 350–360, https://doi.org/10.1007/s00259-020-04771-5.
[4] Y. Hosokawa, et al., Human aiolos, an ikaros-related zinc finger DNA binding protein: cDNA cloning, tissue expression pattern, and chromosomal mapping, Genomics 61 (1999) 326–329, https://doi.org/10.1006/geno.1999.5949.
[5] K. Georgopoulos, et al., The role of the Ikaros gene in lymphocyte development and homeostasis, Annu. Rev. Immunol. 15 (1997) 155–176, https://doi.org/10.1146/annurev.immunol.15.1.155.
[6] S.M. Frisch, M.D. Schaller, The wind god promotes lung cancer, Cancer Cell 25 (2014) 551–552, https://doi.org/10.1016/j.ccr.2014.04.022.
[7] Y. Zou, et al., IKZF3 deficiency potentiates chimeric antigen receptor T cells targeting solid tumors, Cancer Lett. 524 (2022) 121–130, https://doi.org/10.1016/j.canlet.2021.10.016.
[8] Y. Choi, et al., Integrative analysis of oncogenic fusion genes and their functional impact in colorectal cancer, Br. J. Cancer 119 (2018) 230–240, https://doi.org/10.1038/s41416-018-0153-3.
[9] S. Corgnac, et al., CD103+CD8+ TRM cells accumulate in tumors of anti-PD-1-responder lung cancer patients and are tumor-reactive lymphocytes enriched with Tc17, Cell Rep. Med. 1 (2020) 100127, https://doi.org/10.1016/j.xcrm.2020.100127.
[10] X. Li, et al., Aiolos promotes anchorage independence by silencing p66Shc transcription in cancer cells, Cancer Cell 25 (2014) 575–589, https://doi.org/10.1016/j.ccr.2014.03.020.
[11] J. Hung, et al., Overexpression of Aiolos promotes epithelial-mesenchymal transition and cancer stem cell-like properties in lung cancer cells, Sci. Rep. 9 (2019) 2991, https://doi.org/10.1038/s41598-019-39545-z.
[12] M. Saldana, et al., Carraway, Otubain 1: a non-canonical deubiquitinase with an emerging role in cancer, Endocr. Relat. Cancer 26 (2019) R1–R14, https://doi.org/10.1530/ERC-18-0264.

[13] K.J. Livak, T.D. Schmittgen, Analysis of relative gene expression data using real-time quantitative PCR and the 2(-Delta Delta C(T)) Method, Methods 25 (2001) 402–408, https://doi.org/10.1006/meth.2001.1262. PMID: 11846609.
[14] F.J. Guo, et al., Expression and functional characterization of platelet-derived growth factor receptor-like gene, World J. Gastroenterol. 16 (2010) 1465–1472, https://doi.org/10.3748/wjg.v16.i12.1465.
[15] F. Guo, et al., Stanniocalcin1 (STC1) inhibits cell proliferation and invasion of cervical cancer cells, PLoS One 8 (2013) e53989, https://doi.org/10.1371/journal.pone.0053989.
[16] C.C. Liang, A.Y. Park, J.L. Guan, In vitro scratch assay: a convenient and inexpensive method for analysis of cell migration in vitro, Nat. Protoc. 2 (2007) 329–333, https://doi.org/10.1038/nprot.2007.30. PMID: 17406593.
[17] N. Kramer, et al., In vitro cell migration and invasion assays, Mutat. Res. 752 (2013) 10–24, https://doi.org/10.1016/j.mrrev.2012.08.001.
[18] F. Guo, et al., Recent BCR stimulation induces a negative autoregulatory loop via FBXO10 mediated degradation of HGAL, Leukemia 34 (2020) 553–566, https://doi.org/10.1038/s41375-019-0579-5.
[19] Y. Liao, et al., Deubiquitinating enzyme OTUB1 in immunity and cancer: good player or bad actor? Cancer Lett. 526 (2022) 248–258, https://doi.org/10.1016/j.canlet.2021.12.002.
[20] D. Kioussis, Aiolos: an ungrateful member of the Ikaros family, Immunity 26 (2007) 275–277, https://doi.org/10.1016/j.immuni.2007.03.003.
[21] C. Schmitt, et al., Aiolos and Ikaros: regulators of lymphocyte development, homeostasis and lymphoproliferation, Apoptosis 7 (2002) 277–284, https://doi.org/10.1023/a:1015372322419.
[22] A. Zaini, C. Zaph, Aiolos: a molecular guardian of type 2 innate immune cell residency and response, Mucosal Immunol. 14 (2021) 1221–1223, https://doi.org/10.1038/s41385-021-00444-0.
[23] M. Yamashita, et al., A variant in human AIOLOS impairs adaptive immunity by interfering with IKAROS, Nat. Immunol. 22 (2021) 893–903, https://doi.org/10.1038/s41590-021-00951-z.
[24] H.S. Kuehn, et al., Disease-associated AIOLOS variants lead to immune deficiency/dysregulation by haploinsufficiency and redefine AIOLOS functional domains, J. Clin. Invest. 134 (2024) e172573, https://doi.org/10.1172/JCI172573.
[25] M. Yamashita, T. Morio, AIOLOS-associated inborn errors of immunity, J. Clin. Immunol. 44 (2024) 128, https://doi.org/10.1007/s10875-024-01730-9.
[26] T. Shahin, et al., Identification of germline monoallelic mutations in IKZF2 in patients with immune dysregulation, Blood advances 6 (2022) 2444–2451, https://doi.org/10.1182/bloodadvances.2021006367.
[27] M. Cippitelli, et al., Role of aiolos and ikaros in the antitumor and immunomodulatory activity of IMiDs in multiple myeloma: better to lose than to find them, Int. J. Mol. Sci. 22 (2021) 1103, https://doi.org/10.3390/ijms22031103.
[28] L.B. John, A.C. Ward, The Ikaros gene family: transcriptional regulators of hematopoiesis and immunity, Mol. Immunol. 48 (2011) 1272–1278, https://doi.org/10.1016/j.molimm.2011.03.006.
[29] K. Billot, et al., Deregulation of Aiolos expression in chronic lymphocytic leukemia is associated with epigenetic modifications, Blood 117 (2011) 1917–1927, https://doi.org/10.1182/blood-2010-09-307140.
[30] K.H. Hung, et al., Aiolos collaborates with Blimp-1 to regulate the survival of multiple myeloma cells, Cell Death Differ. 23 (2016) 1175–1184, https://doi.org/10.1038/cdd.2015.167.
[31] Z. Zhu, et al., Downregulation of PRDM1 promotes cellular invasion and lung cancer metastasis, Tumour biology 39 (2017), https://doi.org/10.1177/1010428317695929, 1010428317695929.